



Indication of dynamic neurovascular coupling from inconsistency between EEG and fMRI indices across sleep–wake states

Changwei W. Wu^{1,2} · Pei-Jung Tsai^{3,4} · Sharon Chia-Ju Chen⁵ · Chia-Wei Li⁶ · Ai-Ling Hsu⁶ · Hong-Yi Wu⁷ · Yu-Ting Ko⁸ · Pai-Chuan Hung⁸ · Chun-Yen Chang⁹ · Ching-Po Lin¹⁰ · Timothy J. Lane^{1,2} · Chia-Yuen Chen⁶

Received: 24 January 2019 / Accepted: 17 July 2019 / Published online: 2 August 2019
© Japanese Society of Sleep Research 2019

Abstract

Neurovascular coupling (NVC), the transient regional hyperemia following the evoked neuronal responses, is the basis of blood oxygenation level-dependent techniques and is generally adopted across physiological conditions, including the intrinsic resting state. However, the possibility of neurovascular dissociations across physiological alterations is indicated in the literature. To examine the NVC stability across sleep–wake states, we used electroencephalography (EEG) as the index of neural activity and functional magnetic resonance imaging (fMRI) as the measure of cerebrovascular response. Eight healthy adults were recruited for simultaneous EEG–fMRI recordings in nocturnal sleep. We compared the cross-modality (EEG vs. fMRI) consistency of functional indices (spectral amplitude and functional connectivity) among five states of wakefulness and sleep (state effect). We also segregated the brain into three main partitions (anterior, middle and posterior) for spatial assessments (regional effect). Significant state effects were found on δ , α and fMRI indices and regional effects on the α and fMRI indices. However, the cross-state EEG changes in spectral amplitude and functional connectivity did not consistently match the changes in the fMRI indices across sleep–wake states. In spectral amplitude, the δ band peaked at the N3 stage for all brain regions, while the fMRI fluctuation amplitude peaked at the N2 stage in the central and posterior regions. In regional connectivity, the inter-hemispheric connectivity of the δ band peaked at the N3 stage for all regions, but the bilateral fMRI connectivity showed the state changes in the anterior and central regions. The cross-modality inconsistencies across sleep–wake states provided preliminary evidence that the neurovascular relationship may not change in a linear consistency during NREM sleep. Thus, caution shall be exercised when applying the NVC presumption to investigating sleep/wake transitions, even among healthy young adults.

Keywords Neurovascular coupling · Sleep · Electroencephalography (EEG) · Functional magnetic resonance imaging (fMRI) · Spectral power · Functional connectivity

Abbreviations

NVC	Neurovascular coupling
NREM sleep	Non-rapid-eye-movement sleep
EEG	Electroencephalography
fMRI	Functional magnetic resonance imaging
BOLD	Blood oxygenation level-dependent
ALFF	Amplitude of low-frequency fluctuations

AASM	American Academy of Sleep Medicine
CBF	Cerebral blood flow
LFP	Local field potential
AAL	Automated Anatomical Labeling

Introduction

Neurovascular coupling (NVC) refers to the complex neuro-physiological mechanism linking transient neural activities to the local phasic hyperemia following cognitive events. Previously the NVC phenomenon has been derived from the neurophysiological experiments during the task engagement by external stimuli [1–3], and general consensus is achieved that the regional cerebral blood flow (CBF) following neural activities is indicated to be regulated by the multicellular

Electronic supplementary material The online version of this article (<https://doi.org/10.1007/s41105-019-00232-1>) contains supplementary material, which is available to authorized users.

✉ Timothy J. Lane
timlane@tmu.edu.tw

✉ Chia-Yuen Chen
chiayuenchen@gmail.com

Extended author information available on the last page of the article

signaling of vasoactive substances from the neurovascular unit, which comprises neurons, astrocytes and arteriole smooth muscle cells [4–6]. Neurovascular coupling is the key principle of in vivo neuroimaging techniques through blood oxygenation level-dependent (BOLD) hemodynamics [7]. Blood oxygenation level-dependent signals tightly correlates with local field potential (LFP) activities, reflecting the mass neural processes of cortical inputs, in response to visual stimuli [1, 3, 8]. With the support of physiological validations, BOLD-functional magnetic resonance imaging (fMRI) provides favorable spatial correspondence with event-related electrophysiological power over the entire brain [1, 9]. On the basis of NVC, fMRI techniques indirectly measure neural activity and have been widely used to map brain functions across various experimental conditions over the past two decades [10]. Furthermore, NVC is applied not only to investigate evoked brain responses, but also to map intrinsic brain activities or synchronizations, such as sleep [11] or even change of consciousness levels [12].

In contrast to the universal NVC assumption, the literature suggests that NVC is highly sensitive to baseline physiological parameters, denoting disrupted NVC following pathophysiological conditions in mammals [4, 13, 14]. For example, Ma et al. reported dynamic coupling and uncoupling relations between vascular reactivity and membrane potential changes in a rat seizure model [15], and Agarwal et al. demonstrated a neurovascular uncoupling phenomenon in response to motor task among seven patients with de novo brain tumor [16]. The phenomenon of NVC is less consistent than hypothesized, suggesting the NVC depends on the baseline physiological conditions [17].

Rather than pathophysiological conditions, recent studies have focused on the NVC dynamics subject to the varying physiological conditions. They targeted on baseline neuronal activities related to tonic vasoactive mediators, such as adenosine, nitric oxide (NO), and adjacent astrocytes' activities, instead of phasic hyperemia following task engagements [2, 18]. Rosenegger et al. reported that astrocytes provide tonic regulation of arterioles using resting intracellular Ca^{2+} , which is independent of phasic neuronal-evoked vasodilation [19]. In addition to the waking condition, changes in tonic vasoactive mediators in the brain during sleeping have been reported. For example, NO decreases in both rapid eye movement (REM) and non-REM (NREM) sleep [20]. The concentration of adenosine, an inhibitory neuromodulator and vessel dilator, during sleep was approximately 75–80% of that when awake [21]. Frank suggested that the intracellular Ca^{2+} concentrations reached the maximum before sleep and reached the lowest at the end of the sleep period [22]. In brief, the brain experiences substantial changes in neural transmitters, and tonic relationships between neural activities and hemodynamics may be altered during sleep. On the basis of the aforementioned findings, we speculated that

brain NVC dynamically changes across sleep–wake states in normal humans.

To test this speculation, we performed simultaneous acquisition of electroencephalography (EEG) and fMRI to examine the changes in NVC across sleep–wake states, where EEG and fMRI recordings were used as the surrogates for LFP signals and hemodynamic responses, respectively. Studies using the EEG–fMRI fusion technique focused on the indirect linkage between the amplitude of band-limited EEG activity and the large-scale fMRI connectivity [23–25]; however, we conjectured that investigation on NVC should be investigated from the perspective of the same functional index. Therefore, we evaluated the between-modality (EEG/fMRI) consistency of functional indices (including spectral amplitude and regional connectivity) across sleep–wake states in young adults. Specifically, if spontaneous NVC persists stably across sleep–wake conditions, the between-modality indices would fluctuate consistently between the conditions. By contrast, if spontaneous NVC is a time-variant process, a cross-state inconsistency of functional indices would be observed between EEG and fMRI. We used three nocturnal sleep stages (non-rapid-eye-movement or NREM sleep, N1, N2 and N3) and two resting states in wakefulness (before sleep and awakening after sleep) as a dynamic model to test the NVC stability hypothesis.

Materials and methods

We recruited eight young male adults aged from 20 to 27 years (mean age 22.3 ± 2.5 years) with regular sleep duration of 7–8 h per night and consistent bed and wake times for at least 4 days. They had no daytime nap habits, no excessive daytime sleepiness, and no history of neurological or psychiatric disorders. All procedures performed in studies involving human participants were in accordance with the ethical standards of the Institutional Review Board of National Yang-Ming University and with the 1964 Helsinki Declaration and its later amendments or comparable ethical standards. Informed consent was obtained from all individual participants included in the study.

We conducted simultaneous EEG–fMRI recordings in the functional scan. The EEGs were recorded using a 32-channel MR-compatible system (Brain Products, Gilching, Germany), including 30 EEG channels, one electrooculography (EOG) channel and one electrocardiogram (ECG) channel according to the international 10/20 systems. The participant preparation and the entire scan protocol were the same as our previous publication [26]. The simultaneous EEG/fMRI datasets were recorded for three sessions: (1) *Pre-sleep session* for 6 min (144 scans); (2) *Sleeping session* during sleep for at most 125 min. (3) *Awakening session* after sleep for additional 6 min.

Recorded EEG data were preprocessed offline using Analyzer 2.0 (Brain Products). Four electrodes (C3, C4, O1, and O2) were used to determine the sleep stages. The preprocess included down-sampling the EEG signal to 250 Hz, removing the gradient-induced artifact (adaptive average subtraction) and removing the ballistocardiographic artifact using the algorithm based on the R–R interval estimation from the ECG electrode. We used processed EEG recordings for sleep scoring to ensure sleep efficiency in the *Sleeping* session and the arousal level in both the *Pre-sleep* and *Awakening* sessions. A licensed sleep technician from Kaohsiung Medical University Hospital visually scored NREM sleep stages (NREM N1, N2 and N3, where N3 sleep is equivalent to slow wave sleep) for every 30 s frame, in accordance with the criteria of the American Academy of Sleep Medicine (AASM) (Iber, 2007). Subsequently, depending on the sleep scoring outcome, we segregated the consecutive EEG data for at least 5 min in each state, resulting in five segmented EEG datasets corresponding to pre-sleep, N1, N2, N3, and awakening (i.e., the state factor). Subsequently, we segregated the EEG data into five frequency bands for frequency specificity: δ (0.75–4.75 Hz), θ (4.75–8 Hz), α (8–12.5 Hz) and β (12.5–25 Hz) using the finite impulse response filter in EEGLab.

Each frequency band was treated independently for the following spectral and connectivity analyses. In the spectral amplitude, we evaluated two indices for comparison: absolute amplitude (the amplitude integral within predefined frequency bands in EEG and ALFF in fMRI) and relative amplitude (percentage of the absolute amplitude over the integral of the entire brain in EEG and normalized amplitude of low-frequency fluctuations [nALFF] in fMRI). To compromise spatial comparisons between the EEG and fMRI indices, we segregated the scalp channels into three macro-scale lobular sections (anterior, central, and posterior) to obtain region-of-interest (ROI) quantifications (i.e., region factor). For functional connectivity in EEG, we calculated the Pearson's correlation coefficient of various channel pair for each of the frequency bands and constructed a correlation matrix of the brain [27]. We averaged the correlation coefficients within the three brain sections to evaluate the transverse inter-hemispheric connectivity. Additionally, we performed the second spatial division into three intra-hemispheric sections (left, middle, and right side) to assess the intra-hemispheric (longitudinal) communications in the brain.

All fMRI data were preprocessed and analyzed for functional connectivity or fluctuation by AFNI and FSL. In the preprocessing stage, the first four volumes of each session were discarded to achieve a steady state before conducting realignment using rigid body transformation for correcting head motion. The linear trend was removed to eliminate signal drift induced by system instability. The fMRI datasets

were spatially smoothed with a Gaussian kernel (full width at half maximum = 6 mm) and normalized to the standard Montreal Neurological Institute (MNI) template, and resampled to an isotropic resolution of $2 \times 2 \times 2 \text{ mm}^3$. Finally, we performed regressed out nuisance covariates, including six realignment parameters, physiological signals from respiration/cardiac pulsations, and time courses retrieved from the white matter and cerebrospinal fluid. To observe the regional specificity, the brain was parcellated into 90 Automated Anatomical Labeling (AAL) regions. We only selected only 44 AAL surface regions as our ROIs, corresponding to EEG channel locations. We subsequently divided the 44 ROIs into three spatial sections.

In terms of spectral amplitude in fMRI, the voxel-based ALFF analysis was conducted using the voxel-wise Fourier transform, and the square root of the power spectrum across 0.01–0.1 Hz was regarded as the ALFF index [28]. To compensate for the global variations in the whole brain, the nALFF was defined as the value obtained by subtracting the voxel-wise ALFF from the average ALFF of the entire brain, and divided by the standard deviation of ALFF. Both ALFF and nALFF were averaged within three brain regions (anterior, central, and posterior) across five states (pre-sleep, N1, N2, N3, and awakening). In terms of functional connectivity in fMRI, we applied a band-pass filter (0.01–0.1 Hz) on those preprocessed time courses. To examine the inter-regional integrity across the states, we performed the Pearson's correlation analysis on 44 AAL ROIs and constructed a correlation matrix. We averaged the correlation coefficients within three brain regions (anterior, central and posterior) for evaluating the transverse connectivity. We also divided the 44 AAL regions into three parts and quantified the correlation coefficient within the three sections (left, middle and right side) to evaluate the longitudinal intra-hemispheric communication.

In the fMRI group analysis on ALFF indices, we used the one-sample *t* test for each state (FWE-corrected $p < 0.05$). To assess the state and regional effects on the functional indices, a two-way repeated measure analysis of variance (ANOVA; state \times region) was applied to the EEG and fMRI indices separately as the initial step, followed by post hoc *t* tests to estimate the effects of the states separately in each region. Cross-state post hoc comparison was performed using the Bonferroni-corrected paired *t* test at the significance level of $p < 0.05$.

Results

All participants ($n = 8$) reached N3 sleep in the *Sleeping* session, and the individual sleep characteristics are summarized in our previous work [26]. Because we aimed at evaluating spontaneous NVC across sleep–wake states, we specifically

examined cross-state consistency between the functional indices of EEG and fMRI, which can be affected by regional disparities. Accordingly, the functional indices were evaluated in a coarse segregation with three large-scale regions (anterior, middle and posterior areas for inter-hemispheric assessments and left, right and medial areas for longitudinal assessments) in compliance with the sleep literature [29]. The functional indices evaluated were the spectral amplitude and regional connectivity (i.e., temporal synchronizations).

Figure 1 shows the cross-state changes in the integral amplitude of EEG δ , α and fMRI ALFF indices. Results of the θ and β bands were not presented here for overall nonsignificance. The ANOVA results confirmed statistical significances of δ amplitude, α amplitude and ALFF with the regional effect ($F_{4,180} = 14$, $p < 0.011$), state effect ($p < 0.011$) and interactions ($p < 0.023$), except for only the state effect in the α amplitude ($p = 0.45$). Compared with the pre-sleep state, the δ amplitude peaked during N3 sleep (Fig. 1 top panel, $p < 0.002$) and returned to the baseline amplitude after awakening. The state effect was observed for all three regions, and the regional effect depended on the amplitude gap in the central regions. Although the α amplitude (Fig. 1 middle panel, $p = 0.45$) did not show significance in the state effect, the α relative amplitude (Fig. S1) showed region \times state interactions ($p < 0.022$), peaked during N3 sleep in the anterior brain ($p < 0.011$) and valleyed during N3 in the posterior brain ($p < 0.002$). Figure 1 (bottom panel) illustrates the ALFF changes from the fMRI data. The ALFF showed prominent elevations in the central and posterior regions during NREM sleep and peaked during the N2 sleep ($p < 0.001$), inconsistent with the EEG amplitudes. The ALFF in the anterior brain was enhanced during N1 and N2 sleep ($p < 0.002$); however, it reduced to a baseline level during the N3 sleep ($p < 0.005$). On the basis of these significant state effects across sleep–wake states, the cross-state inconsistency between EEG and fMRI was observed in terms of the spectral amplitude.

Figure 2 depicts the changes in the transverse connectivity across the five states, where the longitudinal connectivity is shown in Figure S2. The ANOVA results revealed that δ connectivity showed a regional effect ($p < 0.001$), a state effect ($p < 0.001$) and interactions ($p < 0.025$); α connectivity did not show a state effect ($p > 0.125$); fMRI transverse connectivity showed only a state effect ($p < 0.015$); and fMRI longitudinal connectivity did not present any effect ($p > 0.09$). The δ wave enhanced inter-hemispheric connections along with the sleep depth (Fig. 2; top panel). The bilateral δ connectivity peaked during N3 sleep for the entire brain ($p < 0.001$), but it returned to the baseline level after awakening, regardless of brain regions. Meanwhile, longitudinal δ connections decreased along with sleep depth for both lateral sides ($p < 0.03$), and returned to the baseline level

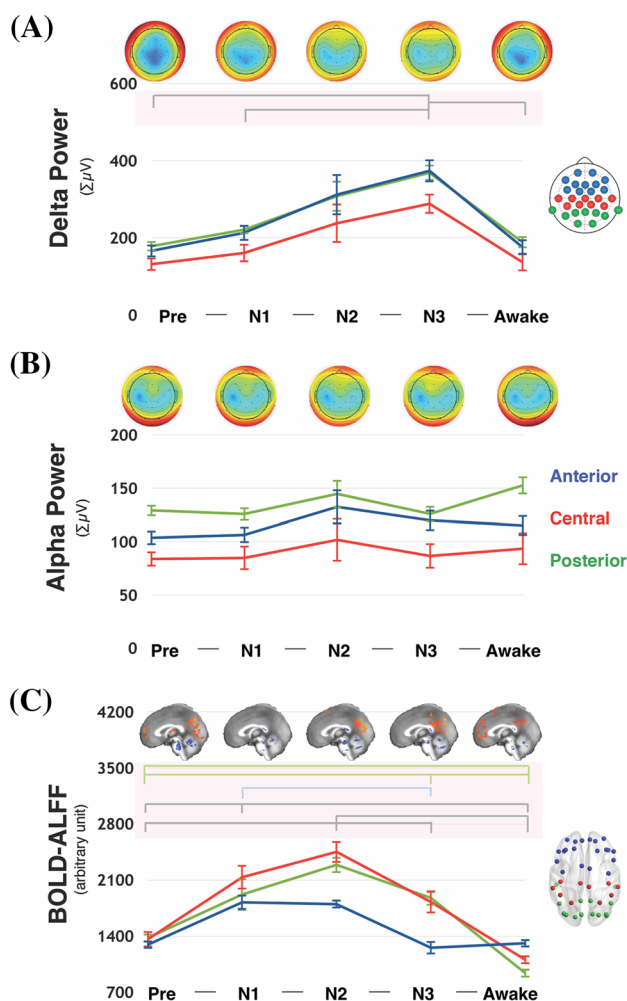


Fig. 1 Dynamic alterations in the spectral amplitude across sleep–wake states. **a** Delta-band topology and the corresponding spectral amplitudes within anterior (blue), central (red) and posterior (green) sections. **b** Alpha-band topology and the corresponding spectral amplitudes within three brain sections. **c** BOLD-ALFF maps and quantified indices within three brain regions, where the ALFF maps were normalized to the whole-brain average. The relative locations of channels (EEG) and ROIs (fMRI) are denoted on the right-hand side. Error bars indicate the standard error. Colored bars in the pink zone denote statistical significance for each paired comparison (two-tailed paired t test with Bonferroni correction $p < 0.05$), where the grey bar represents the common significance of all three regions, blue for the anterior, red for the central, and green for the posterior region (color figure online)

after awakening (Fig. S2). Nevertheless, Fig. 2 (middle panel) shows nonsignificant state effects of the EEG α band in either transverse or longitudinal connections ($p > 0.128$). As shown in the bottom panel of Fig. 2, the central brain showed a lower bilateral connection during the N3 sleep compared with pre-sleep ($p < 0.021$), and the anterior brain showed a trend of increased connectivity during sleep and a significant connectivity drop upon awakening ($p < 0.047$). The BOLD transverse

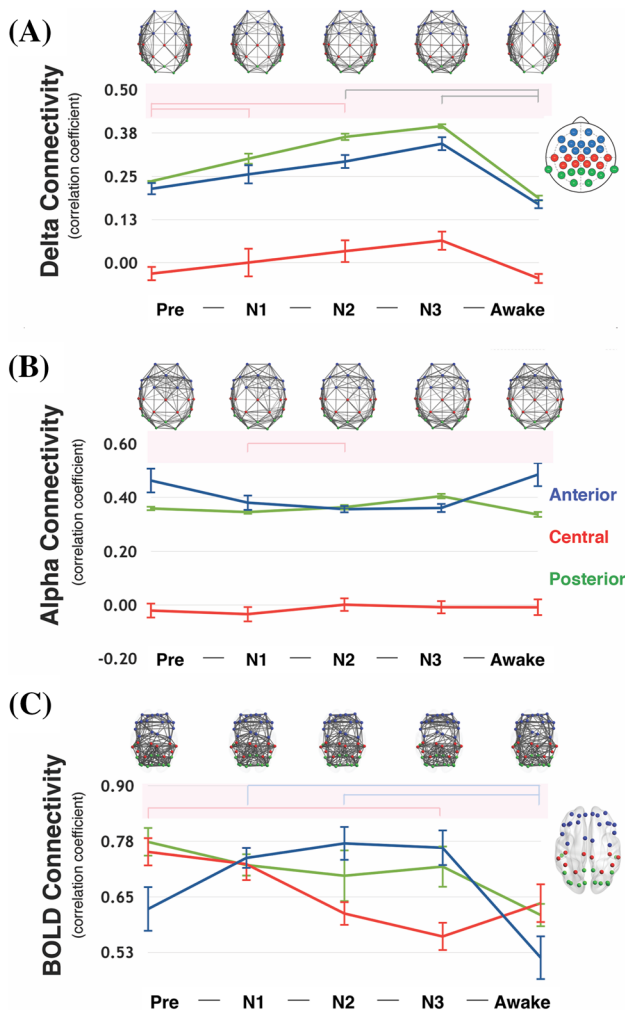


Fig. 2 Dynamic alterations in inter-hemispheric connectivity across sleep–wake states. **a** Delta-band graph patterns and the corresponding cross-channel connectivity within the anterior (blue), central (red), and posterior (green) sections. **b** Alpha-band graph patterns and corresponding cross-channel connectivity within the three brain sections. **c** BOLD-fMRI graph patterns and corresponding cross-region connectivity within three brain regions. Error bars indicate the standard error. Colored bars in the pink zone denote the statistical significances for each paired comparison (two-tail paired *t* test with Bonferroni correction $p < 0.05$), where the grey bar represents the common significance of all three regions, blue for the anterior (or left), red for the central (or medial), and green for the posterior (or right) regions (color figure online)

connectivity did not present significant differences in the posterior brain, and we did not observe significant alterations in fMRI longitudinal connectivity. Finally, with regard to the consistency between EEG and fMRI across the sleep–wake states, the regional connectivity results indicated EEG-fMRI inconsistency across sleep–wake states.

Discussion

The presumption of static neurovascular coupling is applied to the neuroimaging studies for decades, which was recently challenged due to the neurophysiological alterations in clinical patients. The current study is designed to verify whether the NVC is a time-variant process across sleep–wake states in young adults. Results exhibited the cross-state inconsistency between the EEG and fMRI indices (spectral amplitude and functional connectivity), implying the dynamic alterations of neurovascular relationship across sleep–wake states. Specifically, in spectral amplitude, the δ band peaked at the N3 stage for all brain regions, while the ALFF peaked at the N2 stage in the central and posterior regions. In regional connectivity, the inter-hemispheric connectivity of the δ band peaked at the N3 stage for all regions, but the bilateral fMRI connectivity showed the state changes in the anterior and central regions. The cross-state inconsistency of functional indices between EEG and fMRI denote the nonlinear variations of the neurovascular relationship across sleep–wake states, suggesting that the NVC shall not be treated as a constant relation amongst all conditions. Conclusively, we provided preliminary evidence that NVC may deviate based on the alterations of neurophysiological conditions in sleep–wake states, even for healthy young adults.

The majority of neuroimaging studies was performed on the basis of time-invariant NVC assumption; however, the evidence of time-varying NVC is growing. For example, Ma et al. demonstrated in vivo NVC dynamicity along the three stages of epilepsy evolution by using simultaneous intrinsic optical signal and voltages sensitive dye imaging in rat ictal model [15]. Using a sleep-deprived rat model, Schei et al. suggested that prolonged neural activities diminish vascular compliance and limit blood perfusion [30]. Furthermore, Rossenecker et al. suggested the mismatched NVC relationships between task-evoked and ongoing states by demonstrating that astrocytes are involved in the tonic regulation of arterioles using resting intracellular Ca^{2+} , which is independent of neuronal-evoked vasodilation [19]. These findings indicate the possibility of NVC alterations under diverse physiological conditions. Recent reviews on the complex signaling of NVC through several vasoactive substances have reported that the NVC bonding is highly variable and dependent on the baseline physiological condition that are associated with the concentrations of vasoactive factors [4, 6, 7]. One former study conducted by Czisch et al. demonstrated the reduced BOLD responses of auditory stimulation during NREM sleep, providing an evidence of changing physiological conditions during sleep [31]. In the present study, our observations across the sleep–wake states demonstrated

the cross-state inconsistency in the functional indices (spectral amplitude and regional connectivity) between EEG and fMRI. The preliminary results suggest that the transient perturbations of NVC exist not only in patients with cerebrovascular pathologies but also in the alterations of physiological conditions, such as sleep, in healthy young adults. Concerning the possibility that the presumed static NVC becomes a variable, caution should be exercised when conducting neuroimaging investigations.

The NVC assumption was generally adopted by localizing fMRI activations derived from an EEG signature upon specific task engagements. Recent studies used the simultaneous EEG-fMRI recordings to further investigate the variations of NVC in different physiological conditions using visual stimulation tasks [32, 33] or electrical stimulation [17]. Neurovascular relationships in the resting state are generally assumed but rarely investigated. Vazquez et al. found a strong similarity of node-to-node connectivity measured by GCaMP and optical imaging in mice [34]. Shi et al. also found the resting-state BOLD and LFP signals exhibited similar intervoxel correlation profiles in monkeys [35]. These findings support large-scale functional connectivity in both spontaneous neural activity and BOLD hemodynamics, implying the exactness of the NVC assumption in the resting state. However, whether the NVC in the spontaneous activity is static or varying with the physiological conditions remains unclear. Previous studies have suggested that NVC changes depend on physiological conditions. For example, Tarantini et al. showed that the pharmacologically induced disruption of NVC in mice resulted in significant impairment of cognitive functions [36]; Nasrallah et al. used an $\alpha 2$ adrenergic agonist to suppress the inter-hemispheric EEG coherence in rats and reported the preservation of tight NVC [37]; Sumiyoshi demonstrated a significant reduction in stimuli-evoked fMRI responses under mild hypoxic hypoxia in rat, with unchanged EEG responses [17]. Overall, the literature suggests that NVC in spontaneous activity depends on physiological conditions, in support of our expectations in dynamic NVC.

During sleep, the concentrations of neurotransmitters, such as dopamine, gamma-aminobutyric acid, acetylcholine and adenosine, generally deviate across sleep stages, which may force the neurovascular relationship in the normal wakefulness to change in different scenarios and lead to the dynamic NVC in sleep [4]. On the basis of functional connectivity, Massimini et al. demonstrated a breakdown in cortical connectivity by observing rapidly extinguished EEG-evoked responses in NREM sleep without long-range propagation [38]; other fMRI-related studies indicated the reduction of functional connectivity in NREM sleep [11, 12, 39]. These mismatches between the EEG-fMRI indices during sleep might be the consequence

of altered NVC. In the past, the NVC concept is derived from the cerebrovascular reactivity following neural stimuli and was widely adopted to be the basis of neuroimaging investigations over the past two decades. However, the exact physiological function served by the functional hyperemia remains uncertain, and the control mechanism underlying the resting CBF remains elusive [7, 19]. Theoretically among the mathematical models of NVC, the arteriolar compliance (AC) model proposed by Behzadi and Liu is considered capable of fitting BOLD signals in various conditions [7]. In the AC model, the arterioles may generate a dual situation, offering low compliance to CBF at rest and high compliance at activation and creating the NVC disparity for various statuses. The local electrovascular coupling (LEVC) model, developed by Riera and coworkers [6], also introduced the possibility of NVC dynamics by addressing the nonlinear relationship between the extracellular NO concentration (effective vasodilator) and the membrane potentials. During sleep, the membrane potential is regulated between the UP and DOWN states (e.g., in the thalamus), which not only alters the corresponding neural activity [40, 41], but also affects the subsequent perfusion in the LEVC model. Therefore, caution should be exercised when imposing the NVC hypothesis, especially in the spontaneous conditions or sleep stages [19]. We recommend recording peripheral measurements (e.g., heart pulsation, respiration, Galvanic skin response or core body temperature) simultaneously to differentiate participants' baseline physiology for verification, and to more thoroughly understand spontaneous brain activities.

This study had several limitations. First, the sample size was relatively low because of uncontrollable sleep quality inside the MRI scanner for each participant. During the midnight experiment, we could not score the sleep stages during either awakening or sleeping. After the EEG artifact removal and post hoc sleep scoring, we could ensure the pure wakefulness of the pre-sleep and awakening scans and the occurrence of N3 sleep in the eight participants (out of 24 participants). Second, the current results were based on a coarse spatial resolution and the segregation of the brain into three sections (anterior, middle and posterior); this was performed to maintain consistency with previous sleep-associated polysomnography results in literature [29] and to prevent mismatched regional differences between EEG and fMRI. We considered the confounding possibility of large-scale brain segregation on the findings of neurovascular uncoupling; thus, we conducted similar analysis in the part of the EEG channels corresponding to AAL regions in fMRI results (medial prefrontal cortex, precentral gyrus and cuneus). However, the general trend remained the same without significant disparity.

Conclusion

The presumption of static neurovascular coupling is extensively applied to the neuroimaging studies, regardless of the changes in underlying physiological conditions. We tested this assumption across sleep–wake states using simultaneous EEG–fMRI recordings because of dramatic neurophysiological changes during sleep. Results indicated the dynamic alterations of the EEG spectral amplitude (δ and α) and fMRI ALFF across five sleep–wake states, in which the δ amplitude peaked at the N3 sleep while the ALFF peaked at the N2 sleep. Regional connectivity also demonstrated similar mismatched pattern between EEG and fMRI across the sleep–wake states. Such dynamic EEG–fMRI inconsistency (in both spectral amplitude and regional connectivity) across sleep–wake states suggests that the neurovascular relationship does not change consistently in a linear manner across sleep–wake states. The altered neurovascular relation may be raised from the fact that cerebrovascular signaling differs between baseline physiological conditions, implying the existence of multiple condition-dependent neurovascular relationships. Thus, caution shall be exercised when applying the NVC presumption to investigating sleep/wake transitions, even among healthy young adults.

Acknowledgements This research was funded by Taiwan Ministry of Science and Technology (MOST 104-2420-H-038-001-MY3, MOST 105-2628-B-038-013-MY3 and MOST 108-2321-B-038-005-MY2) and Taipei Medical University-Wanfang Hospital research program (107TMU-WFH-17).

Compliance with ethical standards

Conflict of interest Changwei W. Wu declares that he has no conflict of interest. Pei-Jung Tsai declares that she has no conflict of interest. Sharon Chia-Ju Chen declares that she has no conflict of interest. Chia-Wei Li declares that he has no conflict of interest. Ai-Ling Hsu declares that she has no conflict of interest. Hong-Yi Wu declares that she has no conflict of interest. Yu-Ting Ko declares that he has no conflict of interest. Pai-Chuan Hung declares that he has no conflict of interest. Chun-Yen Chang declares that he has no conflict of interest. Ching-Po Lin declares that he has no conflict of interest. Timothy J. Lane declares that he has no conflict of interest. Chen, Chia-Yuen declares that she has no conflict of interest.

Ethical committee permission All procedures performed in studies involving human participants were in accordance with the ethical standards of the Institutional Review Board of National Yang-Ming University and with the 1964 Helsinki Declaration and its later amendments or comparable ethical standards. Informed consent was obtained from all individual participants included in the study.

References

1. Logothetis NK, Pauls J, Augath M, Trinath T, Oeltermann A. Neurophysiological investigation of the basis of the fMRI signal. *Nature*. 2001;412:150–7.
2. Mulert C, Lemieux L, editors. EEG–fMRI: Physiological basis, technique, and applications. Berlin, Heidelberg: Springer. 2009.
3. Scheeringa R, Fries P, Petersson KM, Oostenveld R, Grothe I, Norris DG, et al. Neuronal dynamics underlying high- and low-frequency EEG oscillations contribute independently to the human BOLD signal. *Neuron*. 2011;69:572–83.
4. Girouard H. Neurovascular coupling in the normal brain and in hypertension, stroke, and Alzheimer disease. *J Appl Physiol*. 2006;100:328–35.
5. Attwell D, Buchan AM, Chrapak S, Lauritzen M, MacVicar BA, Newman EA. Glial and neuronal control of brain blood flow. *Nature*. 2010;468:232–43.
6. Riera JJ, Sumiyoshi A. Brain oscillations: ideal scenery to understand the neurovascular coupling. *Curr Opin Neurol*. 2010;23(4):374–381.
7. Huneau C, Benali H, Chabriat H. Investigating human neurovascular coupling using functional neuroimaging: a critical review of dynamic models. *Front Neurosci*. 2015;9:e1002435–12.
8. Magri C, Schridde U, Murayama Y, Panzeri S, Logothetis NK. The amplitude and timing of the BOLD signal reflects the relationship between local field potential power at different frequencies. *J Neurosci Soc Neurosci*. 2012;32:1395–407.
9. Scheeringa R, Koopmans PJ, van Mourik T, Jensen O, Norris DG. The relationship between oscillatory EEG activity and the laminar-specific BOLD signal. *Proc Natl Acad Sci USA*. 2016;113:6761–6.
10. Bandettini PA. Functional MRI: a confluence of fortunate circumstances. *NeuroImage*. 2012;61:A3–11.
11. Horovitz SG, Fukunaga M, de Zwart JA, van Gelderen P, Fulton SC, Balkin TJ, et al. Low frequency BOLD fluctuations during resting wakefulness and light sleep: a simultaneous EEG–fMRI study. *Hum Brain Mapp*. 2008;29:671–82.
12. Tagliazucchi E, Behrens M, Laufs H. Sleep neuroimaging and models of consciousness. *Front Psychol*. 2013;4:256.
13. Pak RW, Hadjiabadi DH, Senarathna J, Agarwal S, Thakor NV, Pillai JJ, et al. Implications of neurovascular uncoupling in functional magnetic resonance imaging (fMRI) of brain tumors. *J Cereb Blood Flow Metab*. 2017;3:271678X17707398–3487.
14. Mikulis DJ. Chronic neurovascular uncoupling syndrome. *Stroke*. 2013;44:S55–7.
15. Ma H, Zhao M, Schwartz TH. Dynamic neurovascular coupling and uncoupling during ictal onset, propagation, and termination revealed by simultaneous in vivo optical imaging of neural activity and local blood volume. *Cereb Cortex*. 2013;23:885–99.
16. Agarwal S, Sair HI, Airan R, Hua J, Jones CK, Heo H-Y, et al. Demonstration of brain tumor-induced neurovascular uncoupling in resting-state fMRI at ultrahigh field. *Brain Connect*. 2016;6:267–72.
17. Sumiyoshi A, Suzuki H, Shimokawa H, Kawashima R. Neurovascular uncoupling under mild hypoxic hypoxia: an EEG–fMRI study in rats. *J Cereb Blood Flow Metab*. 2012;32:1853–8.
18. Raichle ME. The restless brain: how intrinsic activity organizes brain function. *Philos Trans R Soc B: Biol Sci*. 2015;370:20140172–2.
19. Rosenegger DG, Tran CHT, Wamsteeker Cusulin JI, Gordon GR. Tonic local brain blood flow control by astrocytes independent of phasic neurovascular coupling. *J Neurosci*. 2015;35:13463–74.
20. Kostin A, McGinty D, Szymusiak R, Alam MN. Sleep–wake and diurnal modulation of nitric oxide in the perifornical-lateral hypothalamic area: real-time detection in freely behaving rats. *Neuroscience*. 2013;254:275–84.
21. Huston JP, Haas HL, Boix F, Pfister M, Decking U, Schrader J, et al. Extracellular adenosine levels in neostriatum and hippocampus during rest and activity periods of rats. *Neuroscience*. 1996;73:99–107.

22. Frank MG. Astroglial regulation of sleep homeostasis. *Curr Opin Neurobiol.* 2013;23:812–8.
23. Scheeringa R, Petersson KM, Kleinschmidt A, Jensen O, Bastiaansen MCM. EEG α power modulation of fMRI resting-state connectivity. *Brain Connect.* 2012;2:254–64.
24. Tagliazucchi E, von Wegner F, Morzelewski A, Brodbeck V, Laufs H. Dynamic BOLD functional connectivity in humans and its electrophysiological correlates. *Front Hum Neurosci.* 2012;6:339.
25. Chang C, Liu Z, Chen MC, Liu X, Duyn JH. EEG correlates of time-varying BOLD functional connectivity. *NeuroImage.* 2013;72:227–36.
26. Tsai PJ, Chen SCJ, Hsu CY, Wu CW, Wu YC, Hung CS, et al. Local awakening: regional reorganizations of brain oscillations after sleep. *NeuroImage.* 2014;102:894–903.
27. Fraga González G, Smit DJA, van der Molen MJW, Tijms J, Stam CJ, de Geus EJC, et al. EEG resting state functional connectivity in adult dyslexics using phase lag index and graph analysis. *Front Hum Neurosci.* 2018;12:341.
28. Yang H, Long X-Y, Yang Y, Yan H, Zhu C-Z, Zhou X-P, et al. Amplitude of low frequency fluctuation within visual areas revealed by resting-state functional MRI. *NeuroImage.* 2007;36:144–52.
29. Berry RB, Budhiraja R, Gottlieb DJ, Gozal D, Iber C, Kpur VK, et al. Rules for scoring respiratory events in sleep: Update of the 2007 AASM manual for the scoring of sleep and associated events. Deliberations of the sleep apnea definitions task force of the American Academy of Sleep Medicine. *J Clin Sleep Med.* 2012;8(5):597–619.
30. Schei JL, Van Nortwick AS, Meighan PC, Rector DM. Neurovascular saturation thresholds under high intensity auditory stimulation during wake. *Neuroscience.* 2012;227:191–200.
31. Czisch M, Wetter TC, Kaufmann C, Pollmächer T, Holsboer F, Auer DP. Altered processing of acoustic stimuli during sleep: reduced auditory activation and visual deactivation detected by a combined fMRI/EEG study. *NeuroImage.* 2002;16:251–8.
32. Whittaker JR, Driver ID, Bright MG, Murphy K. The absolute CBF response to activation is preserved during elevated perfusion: implications for neurovascular coupling measures. *NeuroImage.* 2016;125:198–207.
33. Fabiani M, Gordon BA, Maclin EL, Pearson MA, Brumback-Peltz CR, Low KA, et al. Neurovascular coupling in normal aging: a combined optical, ERP and fMRI study. *NeuroImage.* 2014;85:592–607.
34. Vazquez AL, Murphy MC, Kim S-G. Neuronal and physiological correlation to hemodynamic resting-state fluctuations in health and disease. *Brain Connect.* 2014;4:727–40.
35. Shi Z, Wu R, Yang P-F, Wang F, Wu T-L, Mishra A, et al. High spatial correspondence at a columnar level between activation and resting state fMRI signals and local field potentials. *Proc Natl Acad Sci USA.* 2017;114:5253–8.
36. Tarantini S, Hertelendy P, Tucsek Z, Valcarcel-Ares MN, Smith N, Menyhart A, et al. Pharmacologically-induced neurovascular uncoupling is associated with cognitive impairment in mice. *J Cereb Blood Flow Metab.* 2015;35:1871–81.
37. Nasrallah FA, Lew SK, Low AS-M, Chuang KH. Neural correlate of resting-state functional connectivity under $\alpha 2$ adrenergic receptor agonist, medetomidine. *NeuroImage.* 2014;84:27–34.
38. Massimini M, Ferrarelli F, Huber R, Esser SK, Singh H, Tononi G. Breakdown of cortical effective connectivity during sleep. *Science.* 2005;309:2228–32.
39. Sämann PG, Wehrle R, Hoehn D, Spormaker VI, Peters H, Tully C, et al. Development of the brain's default mode network from wakefulness to slow wave sleep. *Cereb Cortex.* 2011;21:2082–93.
40. Sherman SM. A wake-up call from the thalamus. *Nat Neurosci.* 2001;4:344–6.
41. Davis B, Tagliazucchi E, Jovicich J, Laufs H, Hasson U. Progression to deep sleep is characterized by changes to BOLD dynamics in sensory cortices. *NeuroImage.* 2016;130:293–305.

Publisher's Note Springer Nature remains neutral with regard to jurisdictional claims in published maps and institutional affiliations.

Affiliations

Changwei W. Wu^{1,2}  · Pei-Jung Tsai^{3,4} · Sharon Chia-Ju Chen⁵ · Chia-Wei Li⁶ · Ai-Ling Hsu⁶ · Hong-Yi Wu⁷ · Yu-Ting Ko⁸ · Pai-Chuan Hung⁸ · Chun-Yen Chang⁹ · Ching-Po Lin¹⁰ · Timothy J. Lane^{1,2} · Chia-Yuen Chen⁶

Changwei W. Wu
sleepbrain@tmu.edu.tw

Pei-Jung Tsai
peijung.tsai77@gmail.com

Sharon Chia-Ju Chen
sharchen@cc.kmu.edu.tw

Chia-Wei Li
chiawei.lee@gmail.com

Ai-Ling Hsu
irene751110@gmail.com

Hong-Yi Wu
w610520@gmail.com

Yu-Ting Ko
kutisjay@hotmail.com

Pai-Chuan Hung
s0911652506@gmail.com

Chun-Yen Chang
changcy@ntnu.edu.tw

Ching-Po Lin
chingpolin@gmail.com

¹ Graduate Institute of Mind, Brain and Consciousness, Taipei Medical University, No. 250, Wu-Xing Street, Xinyi District, Taipei 11031, Taiwan, ROC

² Research Center of Brain and Consciousness, Shuang Ho Hospital, New Taipei, Taiwan

³ Department of Biomedical Imaging and Radiological Sciences, National Yang-Ming University, Taipei, Taiwan

⁴ National Institute on Drug Abuse, National Institutes of Health, Baltimore, USA

⁵ Department of Medical Imaging and Radiological Sciences, Kaohsiung Medical University, Kaohsiung, Taiwan

⁶ Department of Radiology, Wan Fang Hospital, Taipei Medical University, No.111, Sec. 3, Xinglong Rd., Wenshan Dist., Taipei 11696, Taiwan

⁷ Institute of Biomedical Electronics and Bioinformatics, National Taiwan University, Taipei, Taiwan

⁸ Department of Biomedical Sciences and Engineering, National Central University, Taoyuan, Taiwan

⁹ Science Education Center, National Taiwan Normal University, Taipei, Taiwan

¹⁰ Institute of Neuroscience, National Yang-Ming University, Taipei, Taiwan